EMI Shielding Effectiveness Study of a 3D Printed Antenna in Package (AiP)

Dr. Reena Dahle[a], Issa Nesheiwat[a], Roger Murillo[a], Michelle Pirrone[a]

[a]*Division of Engineering Programs, SUNY New Paltz, 1 Hawk Drive, New Paltz NY 12561*

[b]*Sono-Tek Corporation, 2012 Route 9W, Milton, NY 1247, USA*

Abstract

The advancement of communications is driving the requirement for highly dense integrated packaging where the antennas and active electronics are packaged together to form an Antenna-in-Package (AiP) solution. This compact integration can create an interaction, electromagnetic interference (EMI), between the two components highly impacting component-level and system-level performance. To prevent EMI, conductive shielding layers are typically incorporated into the design. The conductivity and method of coating the internal surface used for shielding are important to consider when requiring an effective shield. Standard coating methods such as sputtering, and copper foil can be costly, difficult to realize and non-practical. A new method of ultrasonic spray coating using Sono-Tek's ExactaCoat system with a silver-coated copper and silver particle material, AE5000ST260W7, by Tatsuta is compared to standard coating techniques including copper sputtering and copper tape. Dielectric resonating antennas (DRAs) integrated with a high gain amplifier are tested with and without the presence of the shielding layer and the radiation patterns and radiation efficiency are evaluated. Moreover, the linearity of the amplifier is evaluated by examining the amplifier's output power level as the input power levels to the DRA and amplifier are varied. A total of four additively manufactured DRAs with different conductive layers were tested for their effective EMI shielding: non-Perfect Electric Conductor (PEC), copper tape, sputtered copper, and Tatsuta's conductive ink. The Tatsuta coating provided the most consistent and effective shielding where the amplifier linearity was improved by 6.7dBm over the non-shielded amplifier.

1. Introduction

Standard RF circuits in the sub 6 GHz range generally include antennas that are manufactured discreetly, whether it is milled onto a printed circuit board (PCB) or connected as a separate component with a matching circuit. With the rise of the fifth generation (5G) mobile network, high frequency antennas in the mm-wave will be in much higher demand than ever before [1]. The dramatic shift in frequency reduces the overall footprint of the antenna, which can be assembled into an Antenna in Package (AiP) for a compact and efficient solution.

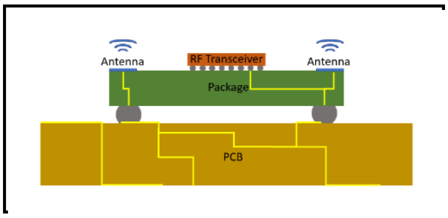

Figure 1: Cross-sectional view of Antenna in Package (AiP) typical implementation.

Higher frequencies require an antenna with high radiation efficiency since standard metallic antennas are considerably less efficient at those frequencies. One solution is to use a dielectric resonator antenna (DRA). The benefit of using dielectric for an antenna is that many different cost-effective materials can be used, from plastics to ceramics [2]. At high frequencies, these DRAs can be made with a small footprint, especially if a material with a high dielectric constant is utilized.

In this case, a rectangular probe fed DRA is integrated with a RF power amplifier to form an AiP. However, this packaging solution introduces the problem of electromagnetic interference (EMI) between the antenna and packaged circuit. One method to mitigate this interference is to add a perfect electric conductor (PEC) layer within the hollow cavity of the antenna, where the amplifier will sit, creating a shielding barrier between the two components.

To reduce the effects of EMI, different materials for the PEC shielding were examined and compared to the performance of an AiP with no PEC. First, 3mil-thick copper tape was used to cover the hollow cavity to recreate the work done in [3] and confirm the results. The next material consisted of sputtered copper, which was deposited in three consecutive layers: 0.5μm of Inconel, 3μm of Cu, and 0.5μm of Inconel. Finally, the last shielding material was an ultrasonic coating of Tatsuta's AE5000ST260W7 EMI shielding material using Sono-Tek's ExactaCoat system.

2. Design, Fabrication and Shielding Materials

2.1. Antenna Design

The DRA antenna is a simple dielectric-based antenna with a resonant frequency of 2.45 GHz, that is determined by the outer and inner dimensions. The antenna is fed by a probe and connected to an SMA connector via a microstrip line, as illustrated in Figure 2(a). The DRA was designed and additively manufactured using a high-k material, Preperm ABS1000 [4]. A hollow cavity was included in the design of the DRA's base to incorporate the amplifier circuit beneath. A 25mil-thick Rogers R03006 RF board, 80mm by 80mm, was used to assemble the AiP with a dielectric constant of 6.5, and a loss tangent of 0.002. Two different antennas were simulated and designed: a DRA with an inner Perfect Electrical Conductor (PEC) layer and one without (non-PEC) along the inner walls of the cavity to simulate the presence and absence of a shielding layer. The dimensions for the non-PEC and PEC antennas are listed in Table 1 below. Dimensions of the hollow cavity were also included. The non-PEC antenna is slightly larger with a longer probe.

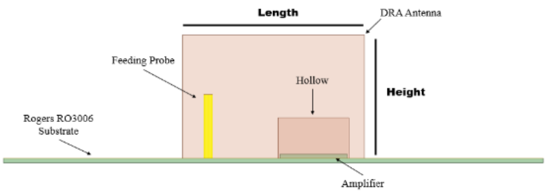

(a)

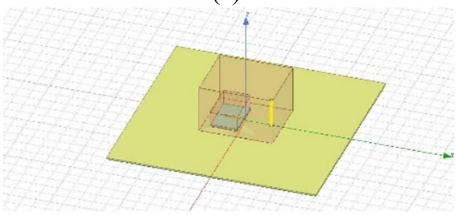

(b)

Figure 2. Overall (a) cross-sectional view of the DRA, and (b) its corresponding isometric view in modeling software.

Table 1. Dimensions of Non-PEC and PEC antenna

Design	Width (mm)	Length (mm)	Height (mm)
Non-PEC Profile	27.6	31	20.3
Non-PEC Hollow	16	10.5	6
Non-PEC Probe	0.65	-	10.75
PEC Profile	23	27	18.3
PEC Hollow	16	11	6
PEC Probe	0.65	-	9.5

2.2. Antenna Fabrication

Preperm ABS1000 is a 3D printing filament material that consists of a high dielectric constant of 10 and a loss tangent of 0.003 at 2.4GHz. The Anet A8 3D printer was used to print this material. To ensure a reliable print, the hot end must be all metal and capable of withstanding temperatures of at least 300°C. Therefore, an all metal E3D V6 hot end and nozzle size of 0.4mm is used. The nozzle temperature was maintained to at least 265°C in order to produce strong layer adhesion. The part cooling fans must be off, and print speeds were reduced to 10-20 mm/s. The material easily warps without proper bed temperatures and preparation, therefore a bed temperature of at least 90°C was maintained during the entire print. The DRA antenna was printed at 100% infill. The 3-D printed antenna is shown in Figure 3.

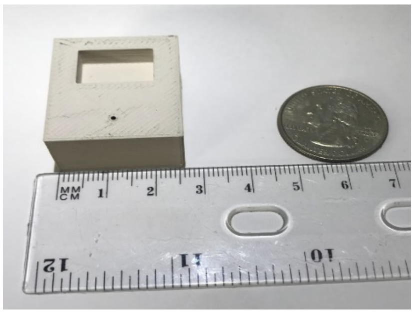

Figure 3. Non-Pec 3D printed DRA using 100% infill Preperm ABS1000.

2.3. Antenna Board Design and Fabrication

The PSA4-5043+ mini circuits amplifier [5] was used for the AiP design. First, the amplifier was simulated using Keysight's ADS software [6] using co-simulation to model the components connected via microstrip lines, as shown in Figure 4(a).

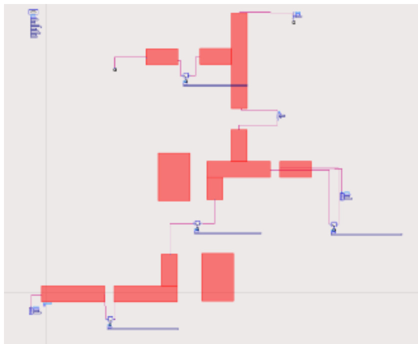

(a)

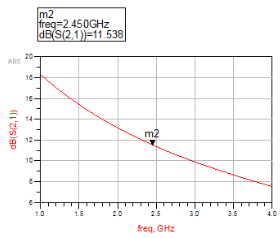

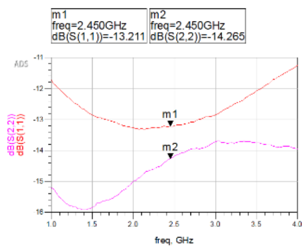

(b) (c)

Figure 4a. Keysight ADS PSA (a) amplifier circuit schematic, and simulated (b) insertion loss S_{21}, and (c) input and output return loss.

The gain of the PSA4-5043+ amplifier is roughly 11.5dB when biased with 5V [5]. As seen in Figure 4(b), the simulation produced 11.54dB of gain. After verifying the circuit, the PCB board layout for the PSA amplifier was created in Eagle [7]. Microstrip lines were used to connect the DRA and the amplifier to each of the ports. Figure 5(a) illustrates the board layout where port 1 was connected to the input of the amplifier, port 2 was connected to the output of the amplifier, and port 3 was connected to the DRA probe feed. With the PCB board layout completed, the board was manufactured and assembled to form the AiP, as shown in Figures 5(b) to 5(d).

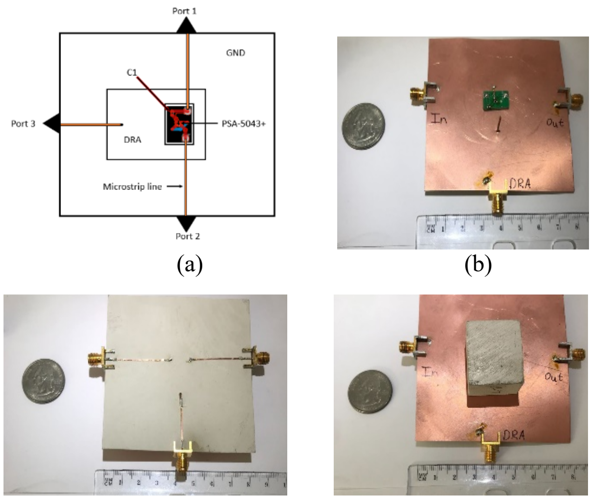

(a) (b) (c) (d)

Figure 5. (a) AiP board layout, (b) top view of the amplifier assembled on the board, (c) bottom view of the assembled board, (d) top view of the final DRA assembled on the board.

2.4. Shielding Materials

Several materials realized via different coating technologies were evaluated for shielding effectiveness along the walls of the hollow cavity within the DRA. The first material investigated was 3 mil-thick copper tape. The copper tape was carefully attached to the hollow cavity and top portion of the DRA, as illustrated in Figure 6(a). The second material evaluated was the sputtered copper using the AJA Orion system. After sample loading, the system is pumped down to a base pressure of 7.3x10^{-7} Torr. 15sccm of UHP argon was used as the sputtering gas. The first deposited layer of Inconel 625 was targeted for 500nm. The deposition time was 3000s at a DC power of 95W.

The copper film had a nominal target of 3um for thickness and was deposited at 100W (DC) over 15000s. The terminating Inconel 625 film was again deposited at 95W of RF power for 3000s (500nm). Post deposition and prior to unload, the system returned to a base pressure of 8.7x10^-7 Torr). This method of sputtering copper material to the 3D printed surface is conformal and will ensure the entirety of the hollow is coated. Although effective, sputtering copper is expensive compared to the overall cost of the antenna and requires to be done at vacuum using highly specialized equipment. Figure 6(b) illustrates the antenna with the sputtered copper. The last material evaluated was a conductive ink from Tatsuta. This coating was ultrasonically coated using a Sono-Tek ExactaCoat system with a 48kHz AccuMist nozzle at a flow rate of 0.2ml/min to achieve a thickness of 6μm. Figure 6(c) illustrates the antenna that was coated at standard flow rate for 12 layers.

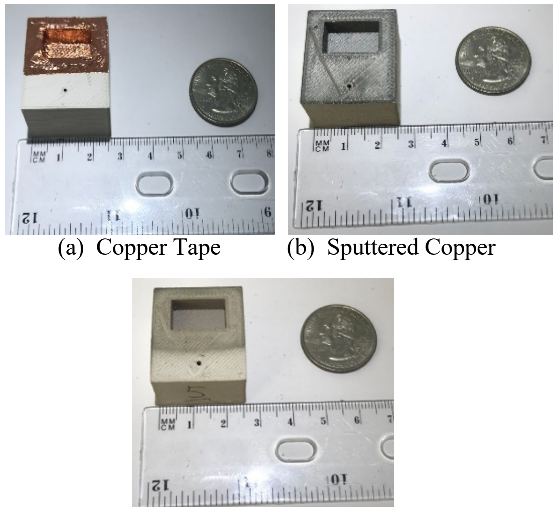

(a) Copper Tape (b) Sputtered Copper

(c) Sono-Tek Spray coated Tatsuta AE5000ST260W7 coating

Figure 6. (a) DRA with copper tape for shielding, (b) Sputtered Inconel-Copper-Inconel, (d) Sono-Tek spray coated Tatsuta Silver coated copper and silver.

Due to the atomizing nature of the Sono-Tek coating technology, the shielding layer produced is a highly conformal layer at room pressure throughout the coated walls of the hollow cavity in the DRA. As seen in Figure 7, an SEM was taken of a cross-section of a coated 3D printed DRA. The filament features peaks and valleys left by the 3D printer and are consistently filled with the Tatsuta AE500ST260W7 material, providing a surface that is fully covered despite the roughness of the surface. Additionally, the vertical portions of the cavity walls are also efficiently coated, leaving a truly conformal coating.

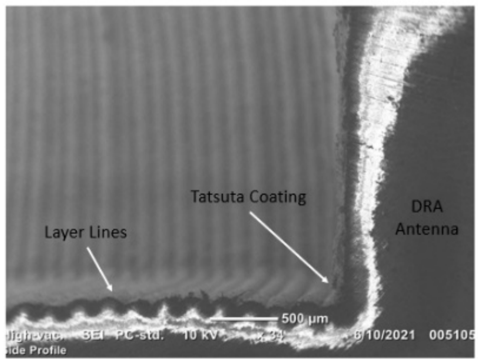

Figure 7. SEM image of the cross-sectional view of a Sono-Tek Tatsuta-coated DRA.

3. Results

To compare the shielding effectiveness of each material, the antenna without any shielding (non-PEC) is measured first to establish a reference. Then, the impact of the presence of the shielding material is evaluated on the DRA's performance in terms of return loss, radiation pattern and gain. Next, the amplifier's linearity performance is evaluated by measuring the gain as the input to the DRA antenna is varied. The antenna that has the least impact on the amplifier's performance, or the amplifier that exhibits the most linear response, is determined to have the best shielding effectiveness

3.1. Antenna Testing

The non-PEC antenna was modeled in electromagnetic simulation software. As seen in Figure 8, the simulated antenna provides a -24dB return loss response at 2.45GHz with a 10dB bandwidth of 11.4%. Compared to the simulated response, the measured non-PEC antenna has a slight shift in frequency. This is a result of additively manufactured variation in the material during the DRA print. Additionally, the measured radiation patterns for the E-field (b) and H-field (c) are shown with simulated patterns and are in good agreement.

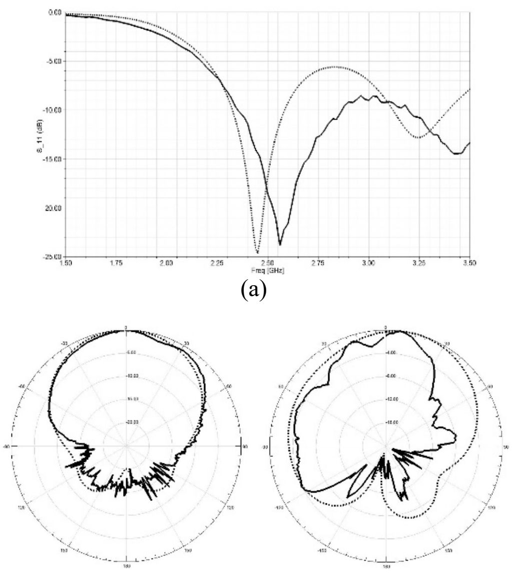
(a)

(b) (c)

Figure 8. Measured (solid) and simulated (dashed) of the non-PEC DRA's (a) return loss S_{11} (dB), and (b) and (c) E and H radiation patterns, respectively.

Next, the PEC DRA antenna was modeled and simulated. Figure 9 represents the simulated return loss in dashed lines with a -33dB loss at 2.45GHz with a bandwidth of 11.02% at 10dB. Compared to the simulated results, the antennas with the other shielding techniques produced similar responses, ensuring minimal impact to return loss performance.

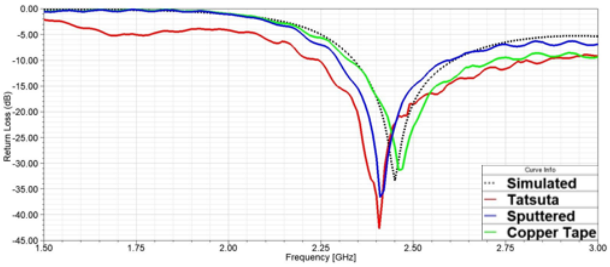

Figure 9. Measured (solid) and simulated (dashed) Return Loss of the PEC DRA.

Additionally, the radiation patterns were simulated and measured. As seen in Figure 10, the PEC coating has little to no effect on the radiation patterns of the antenna.

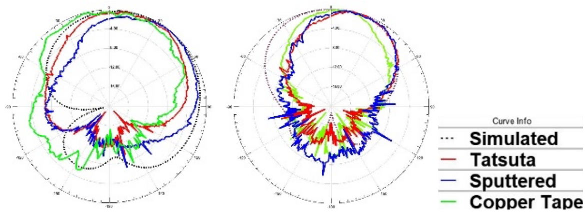

(a) (b)

Figure 10. Measured (solid) and simulated (dashed) Radiation Pattern of the PEC DRA E and H field.

The gain of the antennas was measured and compared to their simulated responses as shown in Table 1. Simulations show that the presence of a shielding material on the cavity wall reduces the DRA gain by up to 1.2dB. The copper tape demonstrated a 2.16dB drop in gain due to the 3mil thickness ($76\mu m$) copper layer. The Sono-Tek ultrasonic spray coated and sputtered DRA demonstrated a closer drop of gain of 0.98dB and 0.68dB, respectively that mimics the drop of gain observed in the simulated models.

Table 2. Measured and Simulated gain of all DRA models.

Gain (dB) @ 2.45GHz	Copper Tape PEC DRA	Sono-Tek PEC DRA	Sputtered PEC DRA	Non-PEC DRA
Measured	1.74	1.92	2.22	2.90
Simulated	3.9	3.9	3.9	5.1

3.2. Amplifier Testing

As input power is increased to an amplifier, the output power is expected to increase linearly. Each DRA with differing shielding materials is analyzed for their shielding effectiveness by evaluating the amplifier's response. Results indicate that the non-PEC antenna performed the worst since the amplifier began to distort when the DRA was fed an input power of 15dBm, as seen in Figure 12.

From 15dBm to 40dBm of input power to the DRA, the amplifier produces a saturated flat output power of about -4.8dBm, while the expected output power should have linearly increased from -25dBm to -5dBm.

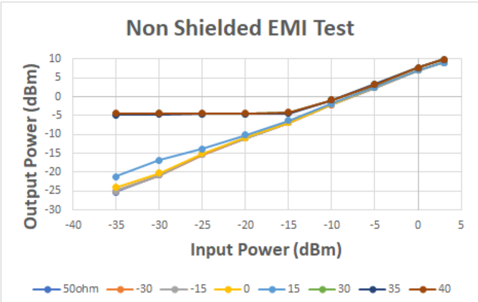

Figure 12. Non-Shielded EMI amplifier linearity response.

As an effort to provide a quick and easy shield at low cost, the copper tape slightly improves the response of the amplifier. In Figure 13, the amplifier still performed worse at a DRA input of 15dBm or higher, but there was a slight improvement in the output power, especially at a DRA input power of 15dBm and 30dBm. The inconsistency in the results can be explained by the difficulty to provide a smooth conformal layer of copper tape.

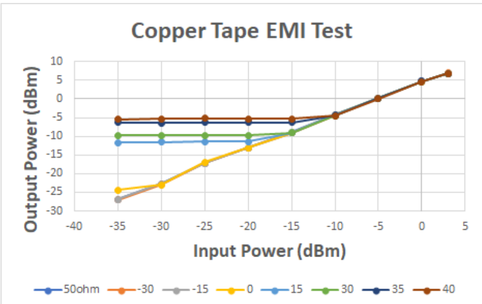

Figure 13. Copper Tape EMI amplifier linearity response.

Sputtering the copper onto the DRA helped improve the shield effectiveness dramatically. Figure 14 represents the measured data from the sputtered copper DRA. Input power to the DRA from 30dBm and above produced an output of -11dBm to -7.5dBm, an improvement over the copper tape and the non-PEC.

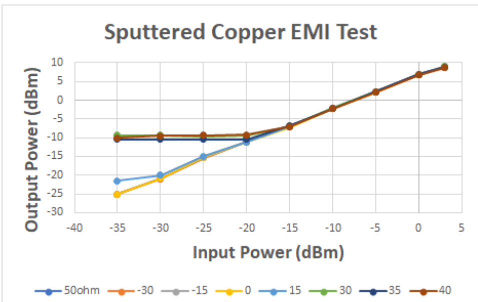

Figure 14. Sputtered Copper EMI amplifier linearity response.

Sono-Tek's Tatsuta coated DRA exhibited the best performance. As seen in Figure 15, a DRA input power of 15dBm and less does not affect the amplifier's linearity. Moreover, at higher DRA input powers, amplifier output response is improved compared to the other designs.

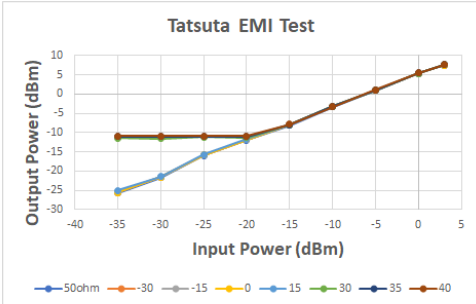

Figure 15. Sono-Tek Tatsuta EMI amplifier linearity response.

4. Conclusion

Incorporating the conductive layer into the hollow of the DRA antenna isolates the antenna from any integrated circuit, minimizing the risk of EMI. However, providing a conformal, smooth, and cost-effective layer of conductive material is essential for an effective shield. As seen in the results presented in this paper, having the right shield will dramatically reduce the amount of electromagnetic interference. Using the Tatsuta material with the ExactaCoat system as a method of shielding provided improved amplifier performance using a simpler and cost-effective approach.

Acknowledgments

The authors would like to thank Sono-Tek for their support in generating the coatings for testing.

References

[1] *Antenna in Package, ASE Group*. [Online]. Available at:<https://ase.aseglobal.com/en/technology/antenna_in_package>
[2] S. Keyrouz and D. Caratelli, "Dielectric Resonator Antennas: Basic Concepts, Design Guidelines at Millimeter-Wave Frequencies," *Int. Journal of Antennas and Propagation*, [Online] 2016, pp.1-20.
[3] S.-J. Guo, K. W. Leung, J.-F. Mao, and N. Yang, "A dielectric resonator antenna-in-package design and its electromagnetic interference investigation on amplifier," *IEEE Access*, vol. 6, pp. 54994–55003, 2018.
[4] 2021. *Preperm ABS1000*. [ebook] Premix, pp.1-2. [Online]. Available: https://www.preperm.com/webshop/wp-content/uploads/2019/03/PREPERM_ABS1000_TDS.pdf. [Accessed 9 June 2021].
[5] 2021. *Monolithic Amplifier PSA4-5043+*. [Online]. Mini-Circuits, pp.1-5. Available: https://www.minicircuits.com/pdfs/PSA45043+.pdf. [Accessed 9 June 2021.
[6] *Advanced Design System*. Keysight. [Online]. Available: https://www.keysight.com/us/en/products/software.html. [Accessed: 9 June 2021].
[7] 2021. *Eagle PCB Design*. Autodesk. [Online]. Available: autodesk.com/products/eagle/overview. Accessed: 9 June 2021.